

Transonic Magnetic Slim Accretion Disks and kilo-Hertz Quasi-Periodic Oscillations in Low-Mass X-Ray Binaries

Dong Lai

Theoretical Astrophysics, California Institute of Technology, Pasadena, CA 91125;
Department of Astronomy, Space Sciences Building, Cornell University, Ithaca, NY 14853;
E-mail: dong@spacenet.tn.cornell.edu

ABSTRACT

The inner regions of accretion disks of weakly magnetized neutron stars are affected by general relativistic gravity and stellar magnetic fields. Even for field strengths sufficiently small so that there is no well-defined magnetosphere surrounding the neutron star, there is still a region in the disk where magnetic field stress plays an important dynamical role. We construct magnetic slim disk models appropriate for neutron stars in low-mass X-ray binaries (LMXBs) which incorporate the effects of both magnetic fields and general relativity (GR). The magnetic field — disk interaction is treated in a phenomenological manner, allowing for both closed and open field configurations. We show that even for surface magnetic fields as weak as $10^7 - 10^8$ G, the sonic point of the accretion flow can be significantly modified from the pure GR value (near $r_{\text{GR}} = 6GM/c^2$ for slowly-rotating neutron stars). We derive an analytical expression for the sonic radius in the limit of small disk viscosity and pressure. We show that the sonic radius mainly depends on the stellar surface field strength B_0 and mass accretion rate \dot{M} through the ratio $b^2 \propto \beta B_0^2 / \dot{M}$, where $\beta \simeq |B_\phi / B_z|$ measures the azimuthal pitch angle of the magnetic field threading the disk. The sonic radius thus obtained approaches the usual Alfvén radius for high b^2 (for which a genuine magnetosphere is expected to form), and asymptotes to $6GM/c^2$ as $b^2 \rightarrow 0$. We therefore suggest that for neutron stars in LMXBs, the distinction between the disk sonic radius and the magnetosphere radius may not exist; there is only one “generalized” sonic radius which is determined by both the GR effect and the magnetic effect.

We apply our theoretical results to the kHz quasi-periodic oscillations (QPOs) observed in the X-ray fluxes of LMXBs. If these QPOs are associated with the orbital frequency at the inner radius of the disk, then the QPO frequencies and their correlation with mass accretion rate can provide useful diagnostics on the (highly uncertain) nature of the magnetic field – disk interactions. In particular, a tight upper limit to the surface magnetic field B_0 can be obtained, i.e., $B_0 \lesssim 3 \times 10^7 (\dot{M}_{17} / \beta)^{1/2}$ G, where $\dot{M}_{17} = \dot{M} / (10^{17} \text{ g s}^{-1})$, in order to produce kHz orbital frequency at the sonic radius. Current observational data may suggest that the magnetic fields in LMXBs have complex topology.

Subject headings: accretion, accretion disks – stars: neutron – X-rays: stars – gravitation – stars: magnetic fields

1. Introduction

The inner region of disk accretion onto neutron stars may be characterized by two unique radii: (i) The marginally stable orbit due to general gravity (GR). For nonrotating neutron stars this is located at

$$r_{\text{GR}} = \frac{6GM}{c^2} = 12.4 M_{1.4} \text{ km}, \quad (1)$$

where M is the neutron star mass, and $M_{1.4} = M/(1.4 M_{\odot})$. For finite rotation rates, r_{GR} is somewhat smaller. The flow behavior near r_{GR} has been subjected to numerous studies, especially in the context of black hole accretion disks (e.g., Muchotrzeb & Paczyński 1982; Matsumoto et al. 1984; Abramowicz et al. 1988; Narayan et al. 1997; Chen et al. 1997): Close to r_{GR} the inward radial velocity of the accreting gas increases steeply with decreasing radius and becomes supersonic. The existence of such marginally stable orbit for neutron star is predicated on the fact that neutron star models constructed using different nuclear equations of state generally give a stellar radius less than r_{GR} (Arnett & Bowers 1977; Kluźniak & Wagoner 1985). (ii) The magnetospheric radius, r_{m} , below which magnetic stress dominates disk plasma stress. While the precise value of r_{m} depends on the (rather uncertain) details of the magnetic field – disk interactions, it is estimated to close to or slightly less than (by a factor of a few) the spherical Alfvén radius, i.e.,

$$r_{\text{m}} \simeq \eta r_{\text{A}} \simeq \eta R \left(\frac{B_0^2 R^3}{\dot{M} \sqrt{GM R}} \right)^{2/7} = 18 \eta R_{10}^{12/7} M_{1.4}^{-1/7} B_8^{4/7} \dot{M}_{17}^{-2/7} \text{ (km)}, \quad (2)$$

with $\eta \lesssim 1$ (e.g., Pringle & Rees 1972; Lamb, Pethick & Pines 1973; Ghosh & Lamb 1979; Arons 1987), where we have scaled various quantities to values appropriate for neutron stars in low-mass X-ray binaries (LMXBs): $R = 10 R_{10}$ km is the neutron star radius, $B_0 = 10^8 B_8$ G is the dipolar surface field strength, and $\dot{M} = (10^{17} \text{ g s}^{-1}) \dot{M}_{17}$ is the mass accretion rate (The Eddington accretion rate is about 10^{18} g s^{-1}). For highly magnetized neutron stars (such as X-ray pulsars, typically having $B \gtrsim 10^{12}$ G), r_{m} is much greater than r_{GR} and the stellar radius, the disk is therefore truncated near r_{m} , within which the disk plasma becomes tied to the closed field lines and is funneled onto the magnetic poles of the star, although some plasma may continue to fall in the equatorial plane as a result of interchange instabilities (Spruit & Taam 1990; see also Arons & Lea 1980). For weakly magnetized neutron stars, such as those expected in LMXBs, r_{m} and r_{GR} are comparable, and the plasma may not climb onto the field lines before reaching the stellar surface. A question therefore arises as to how the magnetic field affects the the dynamics of the inner disk and changes the sonic point. In this paper, we present an unified (albeit phenomenological) treatment of neutron star accretion disks under the combined influences of magnetic fields and strong gravity.

Our study is motivated by the recent observations using the Rossi X-ray Timing Explorer (RXTE) (Bradt, Rothschild & Swank 1993) which revealed kilo-Hertz quasi-periodic oscillations (QPOs) in the X-ray fluxes of at least thirteen LMXBs (see Van der Klis 1997 for a review). These kHz QPOs are characterized by their high levels of coherence (with $\nu/\Delta\nu$ up to 100), large rms amplitudes (up to 20%), and wide span of frequencies (500 – 1200 Hz) which, in most cases, are strongly correlated with the X-ray fluxes. In several sources, the X-ray power spectra show twin kHz peaks moving up and down in frequency together, with the separation frequency roughly constant. Moreover, in five atoll sources single QPOs (with a much higher level of coherence) have been seen during one or more X-ray bursts, with frequencies equal to the frequency differences between the two peaks or twice that. This is a strong indication of beat phenomena (Strohmayer et al. 1996). While the origin of these QPOs is uncertain, it is clear that the action must take place close to the neutron star, either in the accreting atmosphere (Klein et al. 1996) or in the inner disk (Strohmayer et al. 1996; Miller, Lamb and Psaltis 1996). A generic beat-frequency model assumes that the QPO with the higher frequency is associated with the Kepler motion at some preferred orbital radius around the neutron star, while the lower-frequency QPO results from the beat between the Kepler frequency and the neutron star spin frequency. It has been suggested that this preferred radius is the magnetosphere radius (Strohmayer et al. 1996) or the sonic radius of the disk accretion flow (Miller et al. 1996).

In this paper, we are not concerned with the actual mechanisms by which kHz QPOs in the X-ray fluxes of LMXBs may be produced (See Miller et al. 1996 and Van der Klis 1997 for extensive discussion on various possibilities). Rather, our main purpose is to understand what physical effects determine the characteristics of the inner accretion disks in LMXBs. In the sonic-point model, Miller et al. (1996) suggest that some accreting gas can penetrate inside the magnetosphere, whose boundary is located at a larger radius than the sonic radius. For unknown reasons, they assume that these gases are unaffected by the magnetic field once they are inside the magnetosphere and remains in a Keplerian disk. They further suggest that the variation of QPO frequency results from the change in radiative forces on the accretion disk. We note, however, that the effect of radiative forces on the disk fluid (rather than test particle orbiting the central star), is far from clear. Calculating particle trajectories without solving for the global disk structure (M. C. Miller 1997, private communication) is inadequate for determining the magnitude of the radiative forces. While the radiative forces may be important for high-luminosity Z-sources, their effects on the disk dynamics are expected to be small for low-luminosity systems (L less than 10% of L_{Edd}). On the other hand, it is well known that millisecond pulsars have magnetic fields in the range of $10^7 - 10^9$ G, and one expect that neutron stars in LMXBs to have the similar range of field strengths. While the magnetic field may not be strong enough to induce a corotating magnetosphere outside the neutron star, it can nevertheless influence the dynamics of the inner disk flow by transporting away angular momentum from the disk.

Ideally, to properly assess the dynamical effect of magnetic fields on the accretion disks, one needs to solve for both the fluids and the fields self-consistently. This is a difficult task if not

impossible. Despite many decades of theoretical studies (e.g., Pringle & Rees 1972; Lamb et al. 1973; Ghosh & Lamb 1979; Aly 1985, 1991; Arons 1987; Spruit & Taam 1990; Sturrock 1991; Shu et al. 1994; Lovelace et al. 1987, 1995; Stone & Norman 1994; Miller & Stone 1997), there remain considerable uncertainties on the nature of the stellar magnetic field – disk interactions. Particularly outstanding are the issues related to the efficiency of magnetic field dissipation in and outside the disk and whether the stellar field threads the disk in a closed configuration or it becomes open due to differential shearing between the star and the disk. It seems unlikely that some of these issues can be resolved on purely theoretical grounds. In this paper, we shall not attempt a self-consistent magnetohydrodynamics (MHD) calculations. Rather, *we shall adopt a phenomenological approach* and consider rather general field configurations. We believe that such an approach is useful in bridging the gap between full MHD theories and observations. Indeed, as we show in this paper, if the observed kHz QPOs are associated with the sonic point Kepler frequency, then various systematics of kHz QPOs should provide useful constraints on the nature of magnetic field – disk interactions as well as on the magnetic field structure in LMXBs.

In §2 we introduce a model of magnetic slim accretion disk. Numerical solutions are presented in §3. Because of various uncertainties in disk parameters, we shall focus on the simplest models, leaving more complete exploration to future studies. However, in §4 we introduce the notion of “generalized marginally stable orbit” including both the GR and magnetic effects. We derive an analytical expression for the sonic radius, which shows that the sonic point depends mainly on two parameters characterizing the disk magnetic field (in addition to the neutron star mass). We show how different modes of magnetic field – disk interactions can lead to different sonic-point orbital frequencies and their scalings with the field strength and mass accretion rate. Section 5 concerns the equilibrium spin periods of neutron stars in our slim magnetic disk model. Some applications to kHz QPOs in LMXBs are discussed in §6, where we show that our phenomenological approach can be used to learn about the physics of magnetic field – disk interactions.

Unless otherwise noted, we use geometrized units in which the speed of light and Newton’s gravitation constant are unity.

2. Slim Magnetic Accretion Disks

We now consider geometrically thin axisymmetric accretion disk in steady state, taking into account of the transonic nature of the flow, and the deviation from Keplerian motion in the inner region of the disk. Our models generalize the usual “slim disks” around black holes (e.g., Muchotrzeb & Paczyński 1982; Matsumoto et al. 1984; Abramowicz et al. 1988; Narayan et al. 1997; Chen et al. 1997) by including the effect of magnetic fields. GR effects are included in our purely Newtonian treatment by using the pseudo-Newtonian potential introduced by Paczyński & Wiita (1980)

$$\Phi = -\frac{M}{r - 2M}. \quad (3)$$

This potential correctly reproduces the marginally stable orbit ¹ located at $r_{\text{GR}} = 6M$, and is adequate for this initial exploration, considering the much greater uncertainties in the magnetic field – disk interactions. The self-gravity of the disk is neglected.

We assume that the accreting material is confined to a thin disk, and we do not formally introduce a magnetosphere in our model. As discussed in §1, when the field strength is sufficiently high (as in X-ray pulsars, which typically have $B \gtrsim 10^{12}$ G), there is no question that a corotating magnetosphere exists outside the neutron star surface, located near r_m (see Eq. [2]; note that, theoretically, the magnetosphere radius is not known to within a factor of two, nor is it clear what the width of the transition zone is). In such a high-field regime, we shall find that the sonic point as obtained from our model is approximately equal to the usual Alfvén radius. Although in our model the flow continues to be confined in the disk plane even inside the magnetosphere, in reality it may well behave differently (e.g., the plasma may “jump” onto the field lines and get funneled onto the magnetic poles). Thus for high magnetic systems, the supersonic portion of our flow (inside the sonic point) may not be realistic. However, for low magnetic systems (such as LMXBs), which is the main focus of this paper, there needs not be a genuine magnetosphere to truncate the disk flow, but the magnetic forces can still shift the sonic point to a radius larger than $6M$. In such low-field regimes, we expect our global flow solutions to have a wider validity.

2.1. Basic Equations

The mass continuity equation takes the form

$$\dot{M} = -2\pi r \Sigma u, \quad (4)$$

where u is the radial velocity of the flow ($u < 0$ for accretion), and $\Sigma = \int dz \rho \simeq 2H\rho$ is the surface density of the disk. The disk half-thickness ² is given by $H = c_s/\Omega_K$, where $c_s = (p/\rho)^{1/2}$ is the isothermal sound speed, and Ω_K is the Keplerian angular velocity (for the pseudo-Newtonian potential):

$$\Omega_K = \left(\frac{M}{r^3}\right)^{1/2} \frac{r}{r - 2M}. \quad (5)$$

The radial momentum equation reads

$$u \frac{du}{dr} = -\frac{1}{\Sigma} \frac{dP}{dr} + (\Omega^2 - \Omega_K^2)r + \frac{B_z B_r}{2\pi \Sigma} \Big|_{z=H}, \quad (6)$$

¹With small spin parameter $\bar{a} \equiv J/M^2 \ll 1$ (where J is the spin angular momentum), we have $r_{\text{GR}}/M \simeq 6(1 - 0.544\bar{a})$, and $M\Omega_K(r_{\text{GR}}) \simeq 6^{-3/2}(1 + 0.748\bar{a})$. For a spin frequency of 300 Hz (Strohmayer et al. 1996), this amounts to a correction of 7% to r_{GR} and 10% to Ω_K . These corrections are neglected in this paper.

²We neglect the magnetic field effect on the disk thickness. In reality, the disk can be compressed or flattened depending upon the field configuration (see Wang et al. 1990 and Stone & Norman 1994). However, the subsequent analyses in this paper do not depend upon having an explicit expression for H since only height-integrated equations are used.

where $P = \int dz p$ is the integrated disk pressure, Ω is the angular velocity. The last term in Eq. (6) represents the dominant radial magnetic force, obtained by integrating over height the force per unit volume $\partial(B_z B_r / 4\pi) / \partial z$ and dividing by Σ . Note that in Eq. (6), $B_r|_{z=H}$ is evaluated at the upper disk plane, and $B_r|_{z=-H} = -B_r|_{z=H}$. In deriving the magnetic force, we have also neglected the rr -component of the magnetic stress.

The angular momentum equation reads

$$u \frac{dl}{dr} = \frac{r}{\Sigma} \left[\frac{1}{r^2} \frac{d}{dr} \left(r^3 \Sigma \nu \frac{d\Omega}{dr} \right) + \frac{B_z B_\phi}{2\pi} \Big|_{z=H} \right], \quad (7)$$

where the second term on the right-hand-side is the magnetic torque per unit mass, obtained by integrating over height the torque per unit volume $r B_z (\partial B_\phi / \partial z) / 4\pi$ and dividing by Σ . Equation (7) can be integrated in r to give the conservation equation for angular momentum:

$$\dot{M} l_0 = \dot{M} l + 2\pi \nu r^3 \Sigma \frac{d\Omega}{dr} + \dot{M} N_B(r), \quad (8)$$

where l_0 is the integration constant, and

$$\dot{M} N_B(r) = - \int_r^\infty dr r^2 B_z B_\phi \Big|_{z=H}. \quad (9)$$

The three terms on the right-hand-side of Eq. (8) correspond to advective angular momentum transport, viscous torque, and magnetic torque due the threading field lines from r to ∞ , respectively. The constant l_0 is the eigenvalue of the problem; it should be determined by requiring the flow to be regular at the sonic point. We shall adopt the standard α -prescription for the disk kinematic viscosity, i.e., $\nu = \alpha H c_s$ (Shakura & Sunyaev 1973).

The energy equation describing the thermal state of the flow can be written in the form:

$$\Sigma T u \frac{dS}{dr} = \dot{E}_{\text{visc}} + \dot{E}_{\text{Joule}} - 2F_z. \quad (10)$$

Here S is the specific entropy (per unit mass), \dot{E}_{visc} is the viscous heating rate per unit area. With the α -prescription for the disk viscosity, we have

$$\dot{E}_{\text{visc}} = 2H \frac{1}{\rho \nu} \left(\rho \nu r \frac{d\Omega}{dr} \right)^2 = \nu \Sigma \left(r \frac{d\Omega}{dr} \right)^2. \quad (11)$$

The vertical (optically thick) radiative transport flux is

$$F_z = - \frac{c}{3\rho\kappa} \frac{d}{dz} (aT^4) \simeq \frac{caT^4}{\kappa\Sigma}, \quad (12)$$

where κ is the opacity and aT^4 is the radiation energy density. The Joule heating rate \dot{E}_{Joule} depends on the field dissipation in the disk, and its specific form depends on our ansatz for the magnetic field (§2.2).

Finally we need equations of state. For the inner disk region of interest in this paper, radiation pressure dominates over gas pressure. Thus we have $p = aT^4/3$ and $P = 2HaT^4/3$. Also, the opacity is dominated by Thomson scattering, $\kappa = 0.4 \text{ cm}^2/\text{g}$.

2.2. Ansatz for the Magnetic Field

The equations above can be applied to general axisymmetric magnetic field – disk configurations, as long as mass loss from possible disk wind is negligible, and the accreting material is confined to a thin disk plane. We now specify our ansatz for the magnetic fields. The vertical field component is assumed to take the form

$$B_z = B_0 \left(\frac{R}{r} \right)^n. \quad (13)$$

We shall mostly focus on the $n = 3$ case, corresponding to a central stellar dipole field threading the disk (e.g., Ghosh & Lamb 1979; Königl 1991; Yi 1995; Wang 1995), although we will also consider more general values of n , as in the cases when high-order multipoles are important (Arons 1993) or when field lines become open due differential shearing between the disk and the star (Aly 1985, 1991; Sturrock 1991; Newman et al. 1992; Lynden-Bell & Boily 1994; Lovelace et al. 1995). In reality, the power-law relation in Eq. (13) is most likely to be valid only for a small range of r , but as we shall see in §4, the sonic point is mainly determined by the local behavior of the magnetic field.

For the azimuthal component of the magnetic field, we consider two possibilities:

(i) If the stellar magnetic field threads the accretion disk in a closed configurations (e.g., Ghosh & Lamb 1979), then B_ϕ is governed by $\partial B_\phi / \partial t = B_z \partial(r\Omega) / \partial z - B_\phi / \tau$ (where τ is the field dissipation time). In steady-state, this gives $B_\phi \sim \tau(\Omega_s - \Omega)(r/H)B_z$, where Ω_s is the rotation frequency of the star. We define a dimensionless parameter β such that

$$B_\phi \Big|_{z=H} = \beta \left(\frac{\Omega_s - \Omega}{\Omega_K} \right) B_z, \quad (14)$$

where Ω_K is the Kepler frequency and $\Omega (\simeq \Omega_K)$ is the disk orbital frequency. Various (uncertain) estimates for the field dissipation timescale in the magnetically threaded disk configurations have been summarized in Wang (1995).

(ii) If the magnetic field becomes open (e.g., Lovelace et al. 1995), we assume

$$B_\phi \Big|_{z=H} = -\beta B_z, \quad (15)$$

where $\beta \sim 1$ specifies the maximum twist angle of any field line connecting the star and the disk. Clearly, Eq. (14) encompasses the second possibility if we set $\Omega_s = 0$. However, we note that the physical meaning of l_0 in these two cases are rather different: For closed field configurations (i), $\dot{M}l_0$ measures the total torque on the star, while for the (partially) open field configurations (ii), $\dot{M}l_0$ also include the angular momentum carried away from the disk by the magnetic fields of disk outflow. In both cases, $\dot{M}l_0$ is the total angular momentum transported away from the disk per unit time.

Similar to Eq. (14), our ansatz for the radial component B_r of the disk magnetic field is

$$B_r \Big|_{z=H} = \beta_r \left(\frac{-u}{\Omega_K r} \right) B_z. \quad (16)$$

We expect β_r to be of the same order of magnitude as β .

With the particular ansatz for the magnetic fields given by Eq. (14), the Joule heating rate \dot{E}_{Joule} can be calculated as

$$\dot{E}_{\text{Joule}} = \int dz \frac{1}{4\pi} B_z B_\phi \frac{\partial}{\partial z} (r\Omega) = \frac{1}{2\pi} \beta_r B_z^2 \frac{(\Omega_s - \Omega)^2}{\Omega_K}. \quad (17)$$

The dissipation due to the current associated with B_r is much smaller and has been neglected.

3. Numerical Solutions

It is useful to define dimensionless field strengths b and b_r via

$$b^2 = \beta \frac{B_0^2 R^3}{\dot{M} l_R} = 7.317 \beta R_{10}^{5/2} M_{1.4}^{-1/2} \frac{B_8^2}{\dot{M}_{17}}, \quad (18)$$

$$b_r^2 = \beta_r \frac{B_0^2 R^3}{\dot{M} l_R} = 7.317 \beta_r R_{10}^{5/2} M_{1.4}^{-1/2} \frac{B_8^2}{\dot{M}_{17}}, \quad (19)$$

where $l_R \equiv (MR)^{1/2}$. Roughly speaking, b^2 is the ratio of the total magnetic torque and the characteristic accretion torque on the neutron star. Comparing with Eq. (2) we see that for dipole magnetic fields, $r_A/R \sim (b^2/\beta)^{2/7} \sim b^{4/7}$. In all our calculations, we choose $b_r = b$; The flow structure and the sonic radius are rather insensitive to the value of b_r . The radial force equation and the continuity equation can be cast in the form which reveals the existence of a sonic point:

$$\frac{u^2 - a_s^2}{u} \left(\frac{du}{dr} \right) = \frac{a_s^2}{r} + \frac{l^2}{r^3} - \Omega_K^2 r + b_r^2 \frac{u^2 l_R}{r^3 \Omega_K} \left(\frac{R}{r} \right)^{2n-3}, \quad (20)$$

where $a_s^2 \equiv (dP/d\Sigma)_{\text{flow}}$. The sonic point (where $|u| = a_s$) is a critical point of the differential equation. The other equations can also be rewritten in the forms convenient for numerical integration. The angular momentum equation is

$$l_0 = l - \frac{\alpha r^2 c_s^2}{u \Omega_K} \frac{d\Omega}{dr} + N_B, \quad (21)$$

with

$$\frac{dN_B}{dr} = -b^2 \frac{l_R}{r} \left(\frac{R}{r} \right)^{2n-3} \frac{\Omega - \Omega_s}{\Omega_K}. \quad (22)$$

The energy equation is

$$\frac{\Sigma T u}{\dot{M}} \frac{dS}{dr} = -\frac{\alpha c_s^2 r}{2\pi u \Omega_K} \left(\frac{d\Omega}{dr} \right)^2 + \frac{1}{2\pi} b^2 \frac{l_R}{r^2 \Omega_K} \left(\frac{R}{r} \right)^3 (\Omega_s - \Omega)^2 - \frac{3cc_s \Omega_K}{\kappa \dot{M}}. \quad (23)$$

The eigenvalue l_0 is adjusted so that the solution is regular at the sonic point. Equations (20)-(23) are integrated inward from an outer radius (far from the sonic point) where the disk is

approximately Keplerian. Note that in this outer Keplerian region, Eq. (22) can be integrated to give

$$N_B(r) = \frac{b^2 l_R}{2n-3} \left(\frac{R}{r}\right)^{2n-3} \left\{ 1 - \frac{(4n-6)\Omega_s}{(4n-9)(M/r^3)^{1/2}} \left[1 - \frac{(8n-18)M}{(4n-7)r} \right] \right\}, \quad (24)$$

and the angular momentum equation yields

$$u(r) = -\frac{3\alpha r c_s^2}{2(l_K - l_0 + N_B)} \left(\frac{1 - 2M/3r}{1 - 2M/r} \right), \quad (25)$$

where $l_K = r^2\Omega_K$. The sound speed c_s can be obtained from the energy equation (23). Since the radial velocity is small at large radius, the entropy advection term can be neglected. Substituting $\alpha c_s^2/u$ from Eq. (21) into Eq. (23), we find

$$c_s(r) = \frac{\kappa \dot{M} \Omega_K}{4\pi c} \left[\left(1 - \frac{l_0}{l_K} + \frac{N_B}{l_K} \right) \left(\frac{1 - 2M/3r}{1 - 2M/r} \right) + \frac{2}{3} b^2 \frac{l_R}{l_K} \left(\frac{R}{r} \right)^3 \left(1 - \frac{\Omega_s}{\Omega_K} \right)^2 \right]. \quad (26)$$

Equations (20)-(23) turn out to be a rather stiff set of equations. We have opted to adopt a further simplification by assuming the disk is isothermal. We estimate the range of c_s using the thin disk expression (26) evaluated near the sonic radius. The physical rationale behind this approximation is that the transition from Keplerian disk to supersonic flow is very sharp, and we do not expect the sound speed to change significantly in this transition region (near the sonic point). As we shall see in §4, the sonic radius is insensitive to the thermal state of the disk when the sound speed is small. We have not studied the general dependence of the sonic radius on the thermal state of the disk. However, considering the very large uncertainties in the disk magnetic fields, the isothermal approximation should be adequate for use in the first step in our investigation.

Figure 1 depicts two examples of transonic accretion flows, with closed dipolar stellar fields threading the disks ($n = 3$). We choose a standard set of parameters: $\alpha = 0.1$, $c_s = 0.01$, $R/M = 5$ (a typical value for a $M = 1.4 M_\odot$, $R = 10$ km neutron star), and $\Omega_s = 0.013 M^{-1}$ (corresponding to stellar spin frequency of $300 M_{1.4}^{-1}$ Hz). As expected, the magnetic fields slow down the tangential flow velocity, and, together with the strong relativistic gravity, make the radial velocity supersonic at small radii. For small b^2 , the deviation of Ω from Ω_K is small; for larger b^2 , the sonic radius r_s larger, and Ω gradually approaches Ω_s inside the sonic point. In these examples, the sonic points are located at $r_s/M = 7.43$ (for $b^2 = 1$) and 10.95 (for $b^2 = 10$), the corresponding eigenvalues (l_0) are $3.850M$ and $4.153M$, respectively.

In Figure 2 we show the sonic radius r_s and the corresponding specific angular momentum l_0 as a function of b^2 for several different values of α and c_s . We assume $R/M = 5$ and $\Omega_s = 0.013/M$ for these models. The following trends have been found: For a given b^2 , a larger α tends to make r_s larger (i.e., viscosity tends to “destablize” the disk), while a larger c_s tends to make r_s smaller (i.e., pressure “stablizes” the disk). However, we emphasize that dependences of r_s on these disk parameters (α, c_s) are rather weak. Moreover, as c_s decreases, the sonic r_s converges to a value independent of α and c_s — The reason for this convergence will become clear in §4.

4. Analytical Approximation to the Sonic Radius

As our numerical results in §3 indicate, in the limit of small disk pressure and viscosity, the sonic radius approaches a value independent of the disk parameters (α , c_s and the equation of state). This *asymptotic sonic radius* can be derived analytically using a simple mechanical model: Consider the equation of motion of a test mass around a neutron star

$$\frac{d^2 r}{dt^2} = \frac{l^2}{r^3} - \Omega_K^2 r, \quad l_0 = l + N_B(r). \quad (27)$$

Imagine that the test mass is “attached” to a magnetic field line so that its orbital angular momentum l is not conserved by itself. The conserved angular momentum l_0 includes the contributions from both the orbital motion and the angular momentum N_B [cf. Eq. (9)] carried by the threading magnetic field. Equation (27) can be obtained by setting the pressure and viscosity to zero in our general slim disk equations (§2.1). The radial component of the magnetic force has been neglected. An equilibrium orbit is determined by the condition

$$l_0 - N_B = \Omega_K^2 r = l_K(r). \quad (28)$$

Deviation Δr from the equilibrium is governed by the perturbation equation of the form

$$\frac{d^2 \Delta r}{dt^2} + \kappa_{\text{eff}}^2 \Delta r = 0, \quad (29)$$

where the the effective epicyclic frequency κ_{eff} is given by

$$\kappa_{\text{eff}}^2 = \frac{2\Omega_K}{r} \frac{d}{dr} (l_K + N_B) = \frac{M(r - 6M)}{r(r - 2M)^3} - 2b^2 \frac{l_R \Omega_K}{r^2} \left(\frac{R}{r} \right)^{2n-3} \left(1 - \frac{\Omega_s}{\Omega_K} \right), \quad (30)$$

(Recall that $l_R = \sqrt{MR}$ and R is the neutron star radius). Setting $\kappa_{\text{eff}} = 0$, we obtain a critical orbit, which we dub the “*generalized marginal stable orbit*”, located at $r = r_{\text{MSO}}$. Clearly, r_{MSO} depends only on the gravitational potential and the local magnetic torque $(dN_B/dr) = r^2 B_z B_\phi / \dot{M}$. The magnetic field enters only through the dimensionless ratio b . The corresponding constant eigenvalue $l_0 = l_K(r_{\text{MSO}}) + N_B(r_{\text{MSO}})$, however, depends on the global field structure.

In Figure 2 we plot r_{MSO} and l_0 against b^2 for $\Omega_s = 0.013/M$ (corresponding to spin frequency of $300 M_{1.4}^{-1}$ Hz) and $R/M = 5$. We see that r_{MSO} is the upper limit to the numerically determined r_s , i.e., r_{MSO} is the *asymptotic sonic radius as the disk viscosity and pressure diminish*.

It is of interest to consider two limiting cases: (i) In the Newtonian limit (neglecting the GR effect), or equivalently when b^2 is large (so that $r_{\text{MSO}} \gg 6M$), we have

$$\frac{r_{\text{MSO}}}{R} = \left[2b^2 \left(1 - \frac{\Omega_s}{\Omega_K(r_{\text{MSO}})} \right) \right]^{2/(4n-5)}. \quad (31)$$

For $n = 3$, this is the standard result for the inner radius of the Keplerian disk, as determined by $\dot{M}(dl_K/dr) = -r^2 B_z B_\phi|_{z=H}$ (e.g., Arons 1993; Wang 1995); (ii) In the limit of small b^2 (so that

r_{MSO} is close to $6M$), we find

$$\frac{r_{\text{MSO}}}{M} = 6 + \frac{16b^2}{3} \left(\frac{R}{M}\right)^{(4n-5)/2} \left[1 - \frac{\Omega_s}{\Omega_K(6M)}\right]. \quad (32)$$

This gives the correction to the standard general-relativity-induced MSO located at $r_{\text{GR}} = 6M$.

The consideration of the limiting cases clearly indicates the sonic point (or the generalized MSO) constructed in our slim disk model includes the essential physics embodied in the determination of the usual magnetosphere radius. As we argued at the beginning of §2, for high magnetic systems, a genuine magnetosphere should certainly exist outside the neutron star. For low magnetic systems, however, the accretion flow may well be confined in the disk, and the distinction between the sonic point and the magnetosphere boundary may not exist.

We emphasize that our analysis given here is phenomenological. It only takes account of the dynamics of disk under a fixed magnetic field configuration, while a full MHD treatment should include perturbations of both disk fluid and magnetic fields. The usefulness of our analytical result lies in the fact that r_{MSO} provides a good approximation to the sonic radius; and the sonic point is induced by both the GR effect and the magnetic effect. We note that in the presence of disk viscosity and magnetic fields, a fluid element continuously falls inward by the viscous stress and the magnetic stress, and therefore the concept of “marginally stable orbit” does not strictly apply. Nevertheless, we use the term “generalized MSO” to refer to the asymptotic sonic radius as determined by our analytical expressions.

Figure 3 depicts the orbital frequency³ at the generalized MSO (approximately the sonic radius) as a function of the mass accretion rate \dot{M} for several different combinations of model parameters (n and Ω_s). Note that once we specify n and Ω_s in units of $1/M$, the numerical value of r_{MSO}/M depends on the other parameters only through the combination $b^2(R/M)^{(4n-5)/2}$ (see Eqs. [30]-[32]). We have therefore used

$$x = M_{1.4}^{2n-2} R_{10}^{-2n} \frac{\dot{M}_{17}}{\beta B_7^2} = \frac{0.07317}{b^2} \left(\frac{M_{1.4}}{R_{10}}\right)^{(4n-5)/2} \quad (33)$$

as the x -variable in Fig. 3 (where B_7 is the surface field B_0 in units of 10^7 G). For large $\dot{M}/(\beta B_7^2)$ (or small b^2), r_{MSO} approaches $r_{\text{GR}} = 6M$ and $\nu_{\text{MSO}} = \nu_K(r_{\text{MSO}})$ approaches $1.57/M_{1.4}$ kHz. The scaling of ν_{MSO} with \dot{M} depends mainly on n , the index which specifies the shape of the magnetic field lines (see Eq. [13]). Note that the sonic point converges to the MSO only in the limit of small c_s . Thus in reality, the dependence of the sonic-point Kepler frequency $\nu_K(r_s)$ on \dot{M} may be different if c_s is not small. For example, $c_s \propto \dot{M}$ for radiation-dominated optically-thick disk, and therefore the dependence of $\nu_K(r_s)$ on \dot{M} is slightly steeper than what is shown in Fig. 3. We shall discuss some of the applications of Fig. 3 to QPOs in LMXBs in §6.

³To be consistent with the relativistic expression, we use $\nu_{\text{MSO}} = (M/r_{\text{MSO}}^3)^{1/2}/(2\pi)$, rather than the approximate pseudo-Newtonian Eq. (5).

5. Equilibrium Spin Period of Neutron Star

As discussed before (§2.2), for closed field configurations, the quantity $\dot{M}l_0$ measures the total torque on the neutron star due to the accreting matter and the threading magnetic fields. It is of interest to consider how the equilibrium stellar rotation rate $\Omega_{s,eq}$, at which $l_0 = 0$, is determined in the slim disk model. We shall restrict to the dipole fields ($n = 3$) in this section.

First consider the result when the GR effect is neglected. In this case the Keplerian disk boundary r_m is determined by the condition $\dot{M}(dl_K/dr) = -r^2 B_z B_\phi|_{z=H}$, or $\dot{M}l_K(r_m) = 2r_m^3 \beta B_z^2(r_m)(1 - \omega_s)$, where $\omega_s \equiv \Omega_s/\Omega_K(r_m)$. We find

$$\frac{r_m}{R} = \left[2b^2 (1 - \omega_s) \right]^{2/7}, \quad (34)$$

(cf. Eq. [31]). The total torque on the star is given by

$$N_{\text{tot}} = \dot{M}l_0 = \dot{M}l_K(r_m) \frac{7}{6} \left[\frac{1 - (8/7)\omega_s}{1 - \omega_s} \right]. \quad (35)$$

Equilibrium is obtained for $\omega_s = 7/8$. Using Eq. (34) we then find $r_m = (b^2/4)^{2/7} R$ and $\Omega_{s,eq} = (7/8)(M/R^3)^{1/2}(b^2/4)^{-3/7}$, which gives

$$\nu_{s,eq} = 3.44 M_{1.4}^{1/2} R_{10}^{-3/2} b^{-6/7} \text{ (kHz)} = 1.467 M_{1.4}^{5/7} R_{10}^{-18/7} \dot{M}_{17}^{3/7} (\beta B_8^2)^{-3/7} \text{ (kHz)}. \quad (36)$$

This is the standard result that the equilibrium spin frequency is equal to the Keplerian frequency at the Alfvén radius. This result is plotted in Fig. 4.

In the slim magnetic disk model, the total torque on the neutron star $\dot{M}l_0$ is obtained from the eigenvalue l_0 . In the asymptotic regime discussed in §4, l_0 can be determined from the analytical expressions: r_s is obtained from the condition $\kappa_{\text{eff}}^2 = 0$ in Eq. (30), and then $l_0 = l_K(r_s) + N_B(r_s)$ with N_B given by Eq. (24) (specialized to $n = 3$). It is straightforward to show that in the limit of $r \gg M$, we recover the results given in Eqs. (34-36). The equilibrium $\Omega_{s,eq}$ is obtained by requiring $l_0 = 0$. In Fig. 4 we plot the equilibrium spin frequency $\nu_{s,eq}$ as a function of b^2 . Clearly, for large b^2 , our calculation agrees with the usual nonrelativistic result. Relativistic corrections are significant only when b^2 is small, for which the sonic point lies close to the neutron star.

We note that the discussion in this section is valid only if the magnetic fields are closed throughout the disk. Only in these cases does l_0 measure the net torque on the neutron star. Thus our results in this section are much more restrictive compared to the location of the sonic point (which depends only on the local field structure) discussed in §§3-4.

6. Discussion: Applications to QPOs in LMXBs

We have presented in §§2-4 an unified treatment of the inner region of accretion flow under the combined influences of general relativistic gravity and stellar magnetic fields in LMXBs. We

have shown that even relatively weak magnetic fields ($10^7 - 10^8$ G) can slow down the orbital motion in the inner disk by taking away angular momentum from the disk, thereby changing the position of the sonic point significantly (cf. Figs. 2-3).

While the mechanisms responsible for the kHz QPOs in LMXBs are still uncertain, it is tempting to associate them with orbital motions at a certain preferred radius. If this is the case, then the Keplerian frequency at inner radius of the disk, or more precisely the sonic radius is certainly a natural choice (see Paczyński 1987 for an earlier suggestion on the importance of the disk sonic point). One can envisage a number of different mechanisms that will lead to QPOs at $\nu_K(r_s) \simeq \nu_{\text{MSO}}$ and the beat frequency with the stellar spin (Miller et al. 1996; Van der Klis 1997). The following discussion is based on the hypothesis that the kHz QPO frequency corresponds to ν_{MSO} or the sonic-point Kepler frequency. We note that although our treatment of the magnetic field effects in §2-4 is rather general (albeit based on a phenomenological prescription), other physical effects might be at work (such as radiation forces for high-luminosity systems; see §1). As a result, some of our conclusions below should be considered tentative.

(a) *Range of QPO frequencies and constraint on the magnetic field strength:* As emphasized by Van der Klis (1997), similar QPO frequencies (500 – 1200 Hz) have been observed in sources with widely different average luminosities $\langle L \rangle$ (from a few times $10^{-3}L_{\text{Edd}}$ to near L_{Edd} , corresponding to $\langle \dot{M} \rangle$ between a few times 10^{15} g s^{-1} to 10^{18} g s^{-1}), while for an individual source ν_{QPO} often correlates strongly with the X-ray flux. This peculiar lack of correlation between the QPO frequency and $\langle L \rangle$ can be explained in our model, as long as the star’s magnetic field strength correlates with its $\langle \dot{M} \rangle$ in such a way as to leave $\langle \dot{M} \rangle / (\beta B_0^2)$ in a certain range (see Fig. 3). For example, if we use the model with $n = 3$ (dipole field) and $\nu_s = 300$ Hz, then to produce ν_{MSO} in the range of 500 – 1200 Hz would require $0.003 \lesssim \dot{M}_{17} / (\beta B_7^2) \lesssim 0.1$; on the other hand, if we use the model with $n = 2$ and $\nu_s = 0$ (open field configuration), we would require $0.05 \lesssim \dot{M}_{17} / (\beta B_7^2) \lesssim 0.3$ (we have adopted $M_{1.4} = R_{10} = 1$ in these examples). Indeed, such correlation between the magnetic field strength and the mean mass accretion rate among LMXBs has been suggested independently on the basis of Z and atoll source phenomenology (Hasinger & Van der Klis 1989), although the origin for this correlation is still unclear. We note, however, that the correlation needs not be very strong, considering the wide range of other controlling parameters such as n (the shape of the magnetic field) and ν_s (stellar rotation) (see Fig. 3).

While there is a natural upper limit to ν_{MSO} (corresponding to $r_{\text{MSO}} \rightarrow 6M$; but see (c) below), the existence of a (source-dependent) lower limit to the observed QPO frequency needs an explanation. If we rely on inner disk accretion to explain these QPOs (e.g., Van der Klis 1997), then one possibility is that for large r_{MSO} (small ν_{MSO}), the accreting gas can be channeled out of the disk plane by the magnetic field — This must happen for sufficiently small \dot{M} (or sufficiently large B , as in the case of accreting X-ray pulsars). The precise location where the plasma leaves the disk depends on the near-zone field structure, and is clearly source-dependent.

The observed QPO frequencies may already be used to probe the magnetic fields in LMXBs

and the nature of the magnetic field – disk interactions. As an example, consider the atoll source 4U 0614+091 which has extremely small luminosity (see Ford et al. 1997 and references therein): To obtain $\nu_{\text{MSO}} \sim 1150$ Hz requires $\dot{M}_{17}/(\beta B_7^2) \gtrsim 0.1$ (This constraint depends somewhat on the field structure and ν_s ; see Fig. 3). At $\dot{M}_{17} \sim 0.05$, this translates to $\beta^{1/2} B_7 \lesssim 0.7$ — a stronger magnetic field would push the sonic point (or the generalized MSO) to a larger radius. We are left with two possibilities: (i) If $B_7 \gtrsim 10$, we would require $\beta \lesssim 0.01$, i.e., the dissipation of toroidal fields near the disk must be very efficient; (ii) If $\beta \sim 1$ (as expected for open field configurations), then we would require $B_7 \lesssim 1$. Indeed, if the kHz QPO sources represent a fair sample of LMXBs, then we might conclude that the magnetic fields in LMXBs are systematically weaker than those in millisecond pulsars. This may indicate that the magnetic field of a neutron star is “buried” during the LMXB phase (e.g., Romani 1990; Urpin & Geppert 1995; Konar & Bhattacharya 1997; Brown & Bildsten 1998), and later regenerates or re-emerges as accretion stops.

(b) *Scaling of ν_{QPO} with \dot{M}* : For most sources⁴, it was found that the kHz QPO frequency strongly correlates with the XTE count rate (2 – 50 keV), with power-law index greater than unity. However, the scaling relation between the count rate and \dot{M} is not well established, and it has been suggested the flux of the black-body component is a better indicator of QPO frequency (Ford et al. 1997). As discussed in §3, ν_{MSO} depends primarily on the magnetic field structure near the sonic point, particularly on the “field shape” index n . If the scaling of ν_{QPO} with \dot{M} can be established observationally, it may be possible to distinguish a closed field configuration from an open one. For example, if we believe the scaling $\nu_{\text{QPO}} \propto \dot{M}^\sigma$ with $\sigma > 1$, then we may conclude that $n < 2$ (see Eq. [31] and the discussion following Eq. [33]), which indicates that magnetic fields in LMXBs do not have dipolar shape, but rather have complex topology (see Arons 1993 for discussion on related issues).

(c) *The maximum value of ν_{QPO}* : It has been suggested (Zhang et al. 1997) based on the narrow range of the maximal QPO frequencies (1100 – 1200 Hz) in at least six sources that these maximum frequencies correspond to the Kepler frequency at $r_{\text{GR}} = 6M$, which then implies that the neutron star masses are near $2M_\odot$ (see also Kaaret et al. 1997). While we agree that this conclusion seems most natural, we nevertheless add the following cautionary notes: (i) The inferred large stellar masses may be problematic: All neutron stars with well-determined masses (including a few that certainly had accreted mass, although not necessarily in the same accretion mode as in LMXBs) have masses consistent with being $M \simeq 1.4M_\odot$ (e.g., van Kerkwijk et al. 1995). In particular, the 5.4 ms recycled pulsar B1855+09, which is thought to have gone through a LMXB phase (Phinney & Kulkarni 1994), has a mass $1.50 \pm_{0.14}^{0.26} M_\odot$ (Kaspi et al. 1994). Moreover, accretion of $0.6M_\odot$ might have spun up the neutron stars to near break-up (see Cook et al. 1994 for calculations of spin-up tracks in the nonmagnetic case), in contrary to the observed

⁴The possible exceptions are 4U 1608-52 (Berger et al. 1997) and the high-intensity (“banana”) state of 4U 1636-53 (Wijnands et al. 1997), for which the power spectrum shows a single peak with frequency independent of the count rate. However, this may be an artifact of insensitive search of weak QPOs; see Van der Klis (1997).

spin rates (300 – 500 Hz). (ii) If the maximum ν_{QPO} is indeed $\nu_K(6M)$, then the correlation between ν_{QPO} and \dot{M} should weaken as \dot{M} increases, and eventually ν_{QPO} should approach a constant independent of \dot{M} (see Fig. 3). This has not been observed. Therefore in our opinion it is premature to identify the maximal ν_{QPO} with the Kepler frequency at $6M$. An alternative is that as ν_{QPO} approaches 1100 – 1200 Hz, the rms QPO amplitude decreases — as the observations have indicated, making it difficult to detect higher QPO frequencies.

(d) *Horizontal-Branch Oscillations (HBOs) in Z-sources*: In several Z-sources (e.g., Sco X-1, GX 5-1 and GX 17+2), HBOs with frequencies 20 – 50 Hz have been detected *simultaneously* with the kHz QPOs (see Van der Klis 1997). One standard interpretation of HBOs is that they are associated with the beat between the Kepler frequency at the magnetosphere boundary and the neutron star spin (Alpar & Shaham 1985). Since the spin frequencies ν_s of these sources (as determined from the difference in the twin kHz QPO frequencies) lie around 300 Hz (see White & Zhang 1997), the putative magnetosphere boundary must be located at a large radius where $\nu_K \sim \nu_s \sim 300$ Hz. As we have shown in this paper, such a strong magnetic field must necessarily push the (generalized) disk sonic point to a large radius where the Kepler frequency drops below the kilo-Hertz range. (Recall that for low field systems such as LMXBs, the distinction between the sonic point and the magnetosphere boundary probably does not exist, and the two separate radii are replaced by a single generalized sonic point [see §§3-4].) Therefore if the kHz QPOs are associated with the sonic-point Kepler frequency, then the magnetospheric beat frequency model for HBOs cannot work, and the origin of HBOs must lie elsewhere. Alternative models for HBOs have been discussed by Biehle & Blandford (1993) and Stella & Vietri (1997).

The author thanks Zhiyun Li, Rob Nelson and Brian Vaughan for valuable discussions and Lars Bildsten for comment. He also thanks the referee for constructive comments which improved the presentation of the paper. This research is supported by a Richard Chace Tolman Fellowship at Caltech, NASA Grant NAG 5-2756, and NSF Grant AST-9417371.

REFERENCES

- Abramowicz, M. A., Czerny, B., Lasota, J. P., & Szuszkiewicz, E. 1988, ApJ, 332, 646.
- Alpar, A., & Shaham, J. 1985, Nature, 316, 239.
- Aly, J. J. 1985, A&A, 143, 19.
- Aly, J. J. 1991, ApJ, 375, L61.
- Arnett, W. D., & Bowers, R. L. 1977, ApJS, 33, 415.
- Arons, J. 1987, in “The Origin and Evolution of Neutron Stars” (IAU Symp. No. 125), ed. D. J. Helfand & J.-H. Huang (D. Reidel Pub.: Dordrecht).

- Arons, J. 1993, *ApJ*, 408, 160.
- Arons, J., & Lea, S. M. 1980, *ApJ*, 235, 1016.
- Berger, M., et al. 1996, *ApJ*, 469, L13.
- Biehle, G. T., & Blandford, R. D. 1993, *ApJ*, 411, 302.
- Bradt, H. V., Rothschild, R. E., & Swank, J. H. 1993, *A&AS*, 97, 355.
- Brown, E. F., & Bildsten, L. 1998, *ApJ*, in press (astro-ph/9710261).
- Chen, X., Abramowicz, M. A., & Lasota, J.-P. 1997, *ApJ*, 476, 61.
- Cook, G. B., Shapiro, S. L., & Teukolsky, S. A. 1994, *ApJ*, 423, L117.
- Ford, E. C., et al. 1997, *ApJ*, 486, L47 (astro-ph/9706100).
- Ghosh, P., & Lamb, F. K. 1979, *ApJ*, 232, 259.
- Hasinger, G., & Van der Klis, M. 1989, *A&A*, 225, 79.
- Kaaret, P., Ford, E. C., & Chen, K. 1997, *ApJ*, 480, L27.
- Kaspi, V. M., Taylor, J. H., & Ryba, M. F. 1994, *ApJ*, 428, 713.
- Klein, R. I., Arons, J., Jernigan, G., & Hsu, J. 1996, *ApJ*, 457, L85.
- Kluźniak, W., & Wagoner, R. V. 1985, *ApJ*, 297, 548.
- Konar, S., & Bhattacharya, D. 1997, *MNRAS*, 284, 311.
- Königl, A. 1991, *ApJ*, 370, L39.
- Lamb, F. K., Pethick, C. J., & Pines, D. 1973, *ApJ*, 184, 271.
- Lovelace, R. V. E., Wang, J. C. L., & Sulkanen, M. E. 1987, *ApJ*, 315, 504.
- Lovelace, R. V. E., Romanova, M. M., & Bisnovatyi-Kogan, G. S. 1995, *MNRAS*, 275, 244.
- Lynden-Bell, D., & Boily, C. 1994, *MNRAS*, 267, 146.
- Matsumoto, R., Kato, S., Fukue, J., & Okazaki, A. T. 1984, *PASJ*, 36, 71.
- Miller, M. C., Lamb, F. K., & Psaltis, D. 1996, *ApJ*, submitted (astro-ph/9609157).
- Miller, K. A., & Stone, J. M. 1997, *ApJ*, 489, 890.
- Muchotrzeb, B., & Paczyński, B. 1982, *Acta Astr.*, 32, 1.
- Narayan, R., Kato, S., & Honma, F. 1997, *ApJ*, 476, 49.

- Newman, W. I., Newman, A. L., & Lovelace, R. V. E. 1992, *ApJ*, 392, 622.
- Paczyński, B. 1987, *Nature*, 327, 28.
- Paczyński, B., & Wiita, P. 1980, *A&A*, 88, 23.
- Phinney, E. S., & Kulkarni, S. R. 1994, *ARA&A*, 32, 591.
- Pringle, J. E., & Rees, M. J. 1972, *A&A*, 21, 1.
- Romani, R. W. 1990, *Nature*, 347, 741.
- Shakura, N. I., & Sunyaev, R. A. 1973, *A&A*, 24, 337.
- Shu, F. H., et al. 1994, *ApJ*, 429, 781.
- Spruit, H. C., & Taam, R. E. 1990, *A&A*, 229, 475.
- Stella, L., & Vietri, M. 1997, submitted to *ApJ* (astro-ph/9709085).
- Stone, J. M., & Norman, M. L. 1994, *ApJ*, 433, 746.
- Strohmayer, T., et al. 1996, *ApJ*, 469, L9.
- Sturrock, P. A. 1991, *ApJ*, 380, 655.
- Urpin, V. A., & Geppert, U. 1995, *MNRAS*, 275, 1117.
- Van der Klis, M. 1997, in “The Many Faces of Neutron Stars” (Proc. NATO ASI) (astro-ph/9710016).
- Van Kerkwijk, M. H., van Paradijs, J., & Zuiderwijk, E. J. 1995, *A&A*, 303, 497.
- Wang, J. C. L., Sulkanen, M. E., & Lovelace, R. V. E. 1990, *ApJ*, 355, 38.
- Wang, Y.-M. 1995, *ApJ*, 449, L153.
- White, N. E., & Zhang, W. 1997, *ApJ*, 490, L87.
- Wijnands, R. A. D., et al. 1997, *ApJ*, 479, L141.
- Yi, I. 1995, *ApJ*, 442, 768.
- Zhang, W., Strohmayer, T. E., & Swank, J. H. 1997, *ApJ*, 482, L167 (astro-ph/9703151).

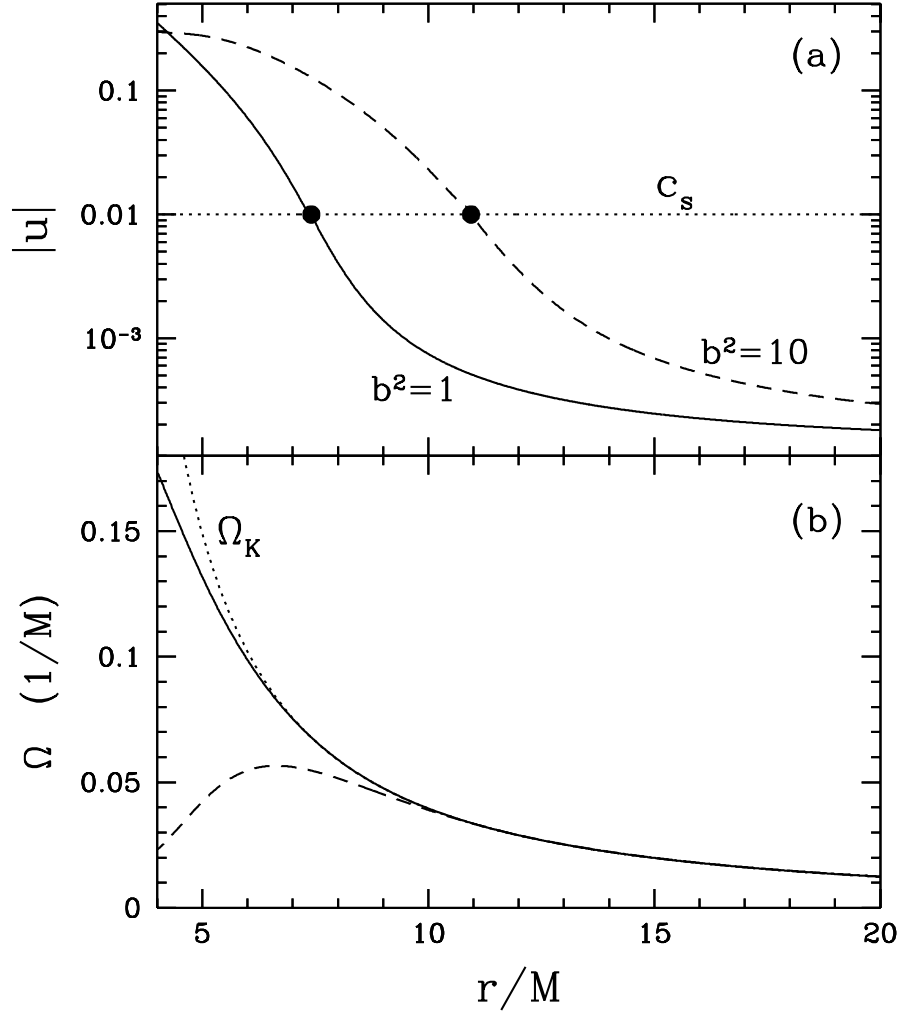


Fig. 1.— (a) Radial velocity $|u|$ (in units of c) and (b) angular velocity Ω (in units of c^3/GM) of transonic accretion flows as a function of disk radii. The model parameters are $n = 3$ (dipolar field), $R/M = 5$, $\alpha = 0.1$, $c_s = 0.01$, $\Omega_s = 0.013/M$, and $b^2 = 1$ (solid curves), 10 (dashed curves). The sonic points are marked by filled circles. The dotted lines depict the sound speed (a) and Keplerian angular velocity (b).

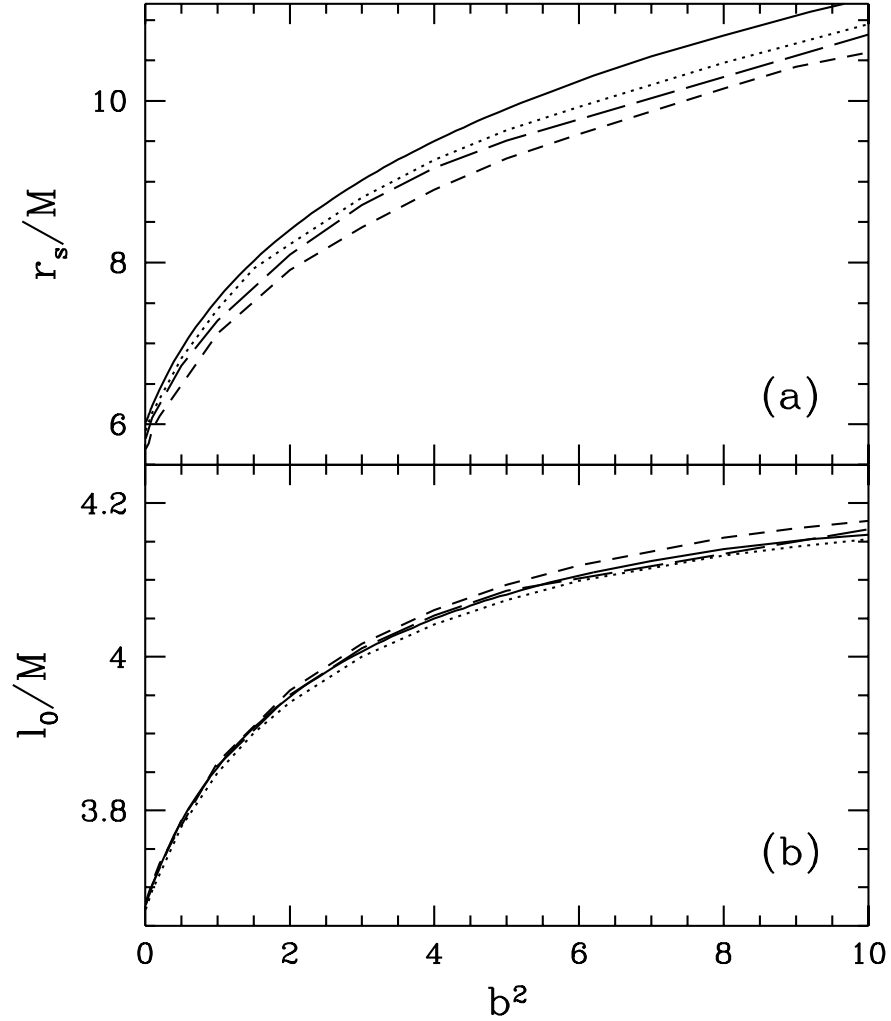


Fig. 2.— (a) The sonic radius and (b) the constant angular momentum l_0 as a function of the dimensionless ratio b^2 (defined in Eq. [18]) for three different models: The dotted lines are for $\alpha = 0.1$, $c_s = 0.01$, the short-dashed lines for $\alpha = 0.02$, $c_s = 0.01$, and the long-dashed lines for $\alpha = 0.02$, $c_s = 0.005$. All models have $n = 3$, $R/M = 5$ and $\Omega_s = 0.013/M$. The solid lines are the asymptotic analytic solutions as discussed in §4.

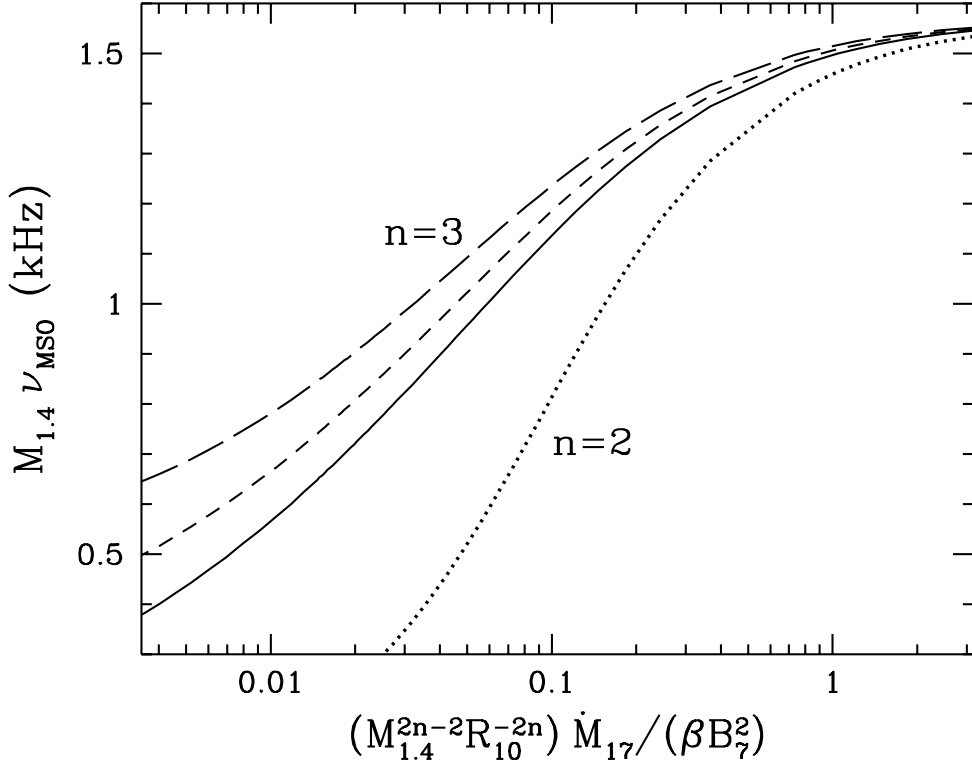


Fig. 3.— Orbital frequency $\nu_{\text{MSO}} = \nu_K(r_{\text{MSO}})$ at the generalized MSO (which approximates the sonic point) as a function of mass accretion rate. The results are obtained using the analytical expressions given in §4. The dotted line corresponds to an open field configuration with $\Omega_s = 0$ and $n = 2$, while the other three lines correspond to closed field configurations with $n = 3$, and $\Omega_s = 0$ (solid line), $0.013/M$ (dashed line), and $0.026/M$ (long-dashed line). Note that for large $\dot{M}/(\beta B_7^2)$ (or small b^2), r_{MSO} approaches $r_{\text{GR}} = 6M$ and ν_{MSO} approaches $1.57/M_{1.4}$ kHz.

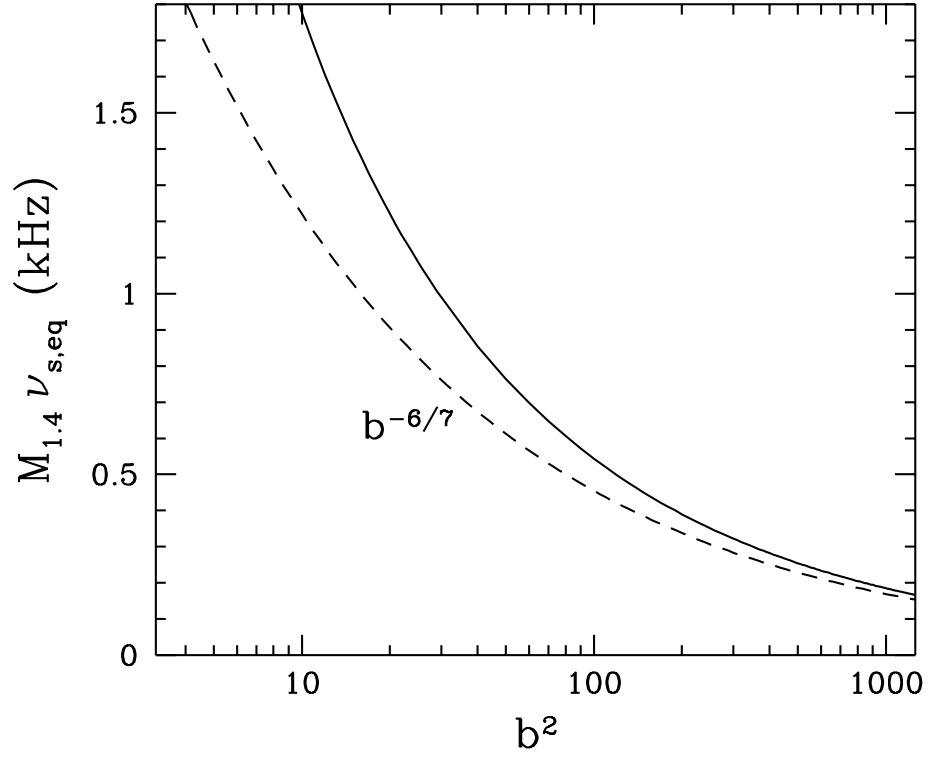


Fig. 4.— The equilibrium spin frequency ν_s of the neutron star as a function of the dimensionless ratio b^2 (defined in Eq. [18]). The solid line is our result including both the GR and magnetic field effects, and the dashed line is usual result as given by Eq. (36).